

examine the nose tip region, the results presented here cover only a small portion of the total length of the vehicle in the axial direction. The physical dimensions of the nose tip as indicated by the sketch in Fig. 1 are the following: initial nose radius (R_n) of 0.5 in., axial length (L), 3.6 in., cone half-angle (δ), 10° , radial coordinate of the cut-off point (R), 0.72 in. It is assumed that this portion of the vehicle is homogeneous and calculations were carried out for beryllium. The trajectory was assumed to be typical for a re-entry vehicle; namely, re-entry velocity of 22,500 fps, re-entry angle of 20° , ballistic parameter of 1000 lb/ft.² It should be pointed out that for the altitude range for which data are presented vehicle slowdown is unimportant. The vehicle is assumed to re-enter the atmosphere at 300 Kft altitude with a uniform initial temperature of 540°R .

For purposes of this calculation it was assumed that the liquid beryllium is immediately removed from the surface after melting and neither the liquid nor the vapor (if vaporized) absorbs any additional heat from the external flowfield.

Fig. 2 shows the ablated shapes at various altitudes. The increase in nose radius is of over 30 times its initial value at 140 Kft. It is also interesting to note the alternate blunting and sharpening of the nose with altitude as the different parts of the body begin to reach melting temperature. It is thus expected that for materials like beryllium, the three-dimensional effects due to coupling between instantaneous heat-transfer rate and body shape become very important.

Fig. 3 shows the isotherms in the nose region at various altitudes. By visualizing lines normal to these isotherms as representing heat-flow direction, one may conclude that thermal conduction is mainly normal to the surface near either the stagnation region or the downstream conical portion of the nose. However, in the intermediate region near the initial sphere-cone junction, heat conduction parallel to the surface becomes important.

IV. Conclusions

The results of this study show that both body-shape change and three-dimensional heat conduction should be considered in the treatment of an ablating, blunt-shaped object. They are necessary for two reasons: a) to account for both radial and axial thermal conduction in the solid, and b) to couple instantaneous body shape with the shape-dependent external heating environment.

Beryllium exhibits major changes in the instantaneous body shape. Severe nose blunting causes a large decrease in the aerodynamic heating rate over the blunted region, thus significantly reducing its recession rate. The portion of the body where the blunted region joins the unmelting part, however, experiences large increases in the heating rate, leading thus to ablation of these corners soon afterwards. The result is a nose-sharpening period during which the radius of curvature decreases and the heating rate in the blunted region increases. These blunting and deblunting periods alternate as different parts of the vehicle undergoes melting. For further details, and an idealized calculation of graphite ablation with axisymmetric heat conduction, the reader is referred to Ref. 6.

References

- 1 Benjamin, A. S., "The Effect of Ablative Geometry Change on the Heating and Recession Characteristics of Sphere-Cones," AIAA Paper No. 66-992, Boston, Mass.
- 2 Karachima, K., Kubota, H., and Sato, K., "An Aerodynamic Study of Ablation Near the Region of Stagnation Point of Axially Symmetric Bodies at Hypersonic Speeds," Rept 425, 1968, Institute of Space and Aeronautical Science, University of Tokyo, Tokyo, Japan.
- 3 Landau, H. G., "Heat Conduction in a Melting Solid," *Quarterly of Applied Mathematics*, Vol. 8, No. 81, 1950.
- 4 Lees, L., "Laminar Heat Transfer Over Blunt Nosed Bodies at Hypersonic Flight Speeds," *Jet Propulsion*, Vol. 26, April 1956, pp 259-269.

⁵ Feldman, S., "Hypersonic Gas Dynamic Charts for Equilibrium Air," Avco Research Rept. 40, Jan. 1957.

⁶ Popper, L. A., Toong, T. Y., and Sutton, G. W., "Axisymmetric Ablation with Shape Changes and Internal Heat Conduction," AIAA Paper No. 70-199, New York, 1970.

Laser Schlieren Crossed-Beam Measurements in a Supersonic Jet Shear Layer

B. H. FUNK* AND K. D. JOHNSTON*

NASA Marshall Space Flight Center, Huntsville, Ala.

Nomenclature

e	= deviation from time-averaged signal voltage
N_o	= ambient index of refraction
S	= schlieren sensitivity
t	= time
U	= flow speed
x, y, z	= nozzle-fixed coordinates (Fig. 1)
α	= Gladstone-Dale constant
ξ, η, ζ	= beam-fixed coordinates (Fig. 1)
ρ	= density
ρ'	= deviation from time-averaged density
τ	= time lag
τ_p	= time lag at which maximum correlation occurs

Subscripts

c	= convection
e	= nozzle exit
H	= horizontal beam
V	= vertical beam

Introduction

THE optical crossed-beam technique has heretofore been used to measure statistical properties of turbulent flow by monitoring the fluctuations in light intensity caused by random fluctuations of the absorption or scattering coefficients.^{1,2} Local information is retrieved by cross correlating the random outputs of two photodetectors that measure the fluctuating intensity of two mutually perpendicular light beams.

In addition to absorption and scattering, index of refraction fluctuations can also produce signal fluctuations; however, in the previous ultraviolet absorption crossed-beam experiments, this effect was minimized by the optical design. The potency of the schlieren effect for crossed-beam measurements

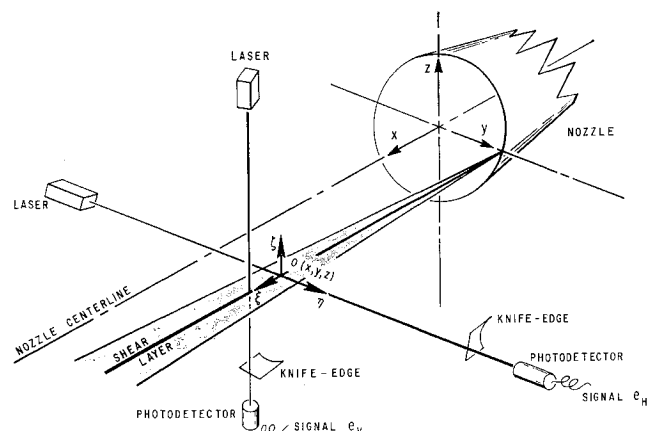


Fig. 1 Laser schlieren crossed-beam arrangement.

Received July 16, 1970.

* Aerospace Engineers.

was realized while attempting to operate a laser beam system in the visible spectrum ($\lambda = 6328 \text{ \AA}$) by employing tracer particles to produce scattering. It was found that the schlieren effect predominated over the scattering even though no knife edges were in the beams. This was attributed to the beam cross-section moving about on the edge, or surface of nonconstant sensitivity, of the photodetector. Introduction of knife edges in the beams increased the signal levels and the two-beam covariance. The initial experiments are described in Ref. 3, and the effect of rotation of the turbulent structures is discussed in Ref. 4. This Note presents the results from a feasibility test of the laser schlieren crossed-beam technique in a supersonic jet.

Technique

The laser schlieren technique seems to be more promising than a system based on absorption or scattering because 1) the sensitivity of the schlieren system can be adjusted to permit measurement of much smaller fluctuations than is possible with the other two systems and 2) the schlieren signals are more directly related to a property of the flow, i.e., density. The test arrangement is shown in Fig. 1. The knife edges are positioned to intercept half the light of the undeflected beams. The covariance of the signals from the two beams is related to the density fluctuations as follows:

$$G(x + \xi, y, z, \tau) = \langle e_{HeV} \rangle = \frac{\alpha^2 S_H S_V}{N_0^2} \int_{-\infty}^{\infty} \int_{-\infty}^{\infty} \left\langle \frac{\partial \rho'(x, y + \eta, z, t + \tau)}{\partial x} \frac{\partial \rho'(x + \xi, y, z + \zeta, t)}{\partial x} \right\rangle d\eta d\zeta \quad (1)$$

The integrand is the covariance of $\partial \rho / \partial x$ at two points, one on each beam. The covariance is appreciable only if the two points are separated by less than an integral length scale. Therefore, the contributions to $\langle e_{HeV} \rangle$ come from a correlation volume centered about the beam intersection point; the point pairs close to the intersection point contribute more than those farther away. Thus, the covariance $\langle e_{HeV} \rangle$ is determined by the magnitude of the fluctuations of $\partial \rho / \partial x$ near the beam intersection point and the size of the correlation volume. A crude interpretation of Eq. (1), which is sufficient for these preliminary results, can be given for zero beam separation and zero time lag as done in Ref. 2.

$$G(x, y, z, \tau = 0) = (\alpha^2 S_H S_V / N_0^2) \langle [\partial \rho'(x, y, z) / \partial x]^2 \rangle \times A(x, y, z) \quad (2)$$

where $A(x, y, z)$ is the cross-sectional area, in the plane of the beams, of the correlation volume which is centered at the beam intersection point. Similarly, a crude approximation of the space-time correlation coefficient between two points separated by a distance ξ in the streamwise direction can be obtained from separated beams as done in Ref. 1.

$$r(\xi, \tau) = [G(x + \xi, y, z, \tau) / G(x, y, z, \tau = 0)] \quad (3)$$

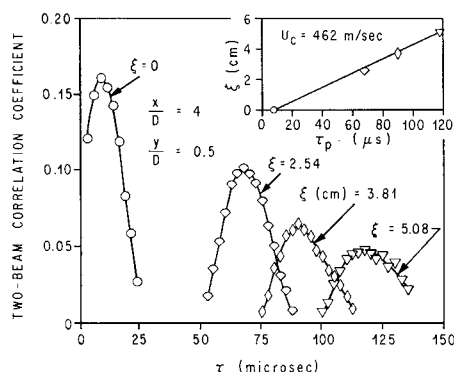


Fig. 2 Two-beam space-time correlations.

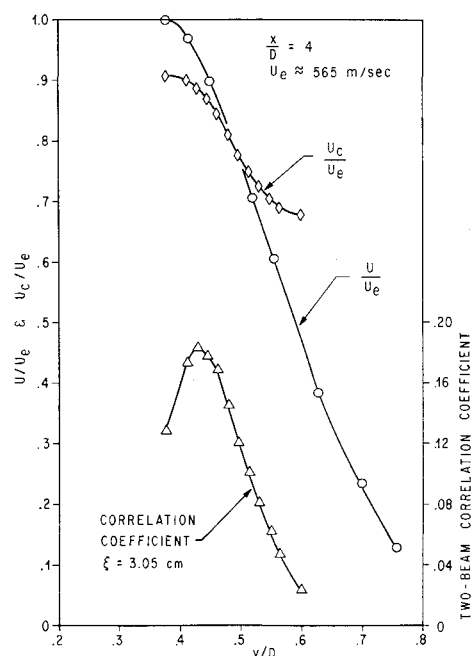


Fig. 3 Convection speed, mean speed, and maximum correlation coefficient profiles.

Experiment

The measurements were made in the shear layer of a shock-free, Mach 2.46 jet which is described in Ref. 2. The nozzle exit diameter D was 7.42 cm. The two-beam correlation coefficient is shown in Fig. 2 for four beam separations with the point "0" (Fig. 1) at $x/D = 4$, $y/D = 0.5$. Following customary practice, the two-beam covariance, $G(x + \xi, y, z, \tau)$, is normalized by the product of the rms values of e_H and e_V rather than by $G(x, y, z, \tau = 0)$. The convection speed is obtained in the inset of Fig. 2 by plotting beam separation vs the time lag at which the peak correlation occurs, τ_p , and then taking the slope of the best straight line fit through these points.

The convection speed profile in the shear layer at $x/D = 4$ is shown in Fig. 3. These convection speeds were obtained using only one beam separation, $\xi = 3.05$ cm. The points from the outer part of the shear layer are in the intermittent zone where the meaning of crossed-beam measurements is not well understood; therefore, not much credence should be put in the outermost points. Furthermore, all the measured convection speeds could be in error because of the effect of rotation of the turbulent structures.⁴ The mean speed profile from Ref. 2 is shown for comparison.

The two-beam correlation coefficient curve for a beam separation of 3.05 cm and $\tau = \tau_p$ is also given in Fig. 3. Although this curve was not obtained with intersecting beams, it probably gives a good indication of the shape of the mean square $\partial \rho' / \partial x$ profile, as might be inferred from Eq. (2).

References

- 1 Fisher, M. J. and Krause, F. R., "The Crossed-Beam Correlation Technique," *Journal of Fluid Mechanics*, Vol. 28, Part 4, 1967, pp. 705-717.
- 2 Fisher, M. J. and Johnston, K. D., "Turbulence Measurements in Supersonic, Shock-Free Jets by the Optical Crossed-Beam Method," TN D-5206, 1970, NASA.
- 3 Funk, B. H. and Cikanek, H. A., "Optical Probing of Supersonic Aerodynamic Turbulence with Statistical Correlation. Phase 1: Feasibility," TM X-53850, 1969, NASA.
- 4 Funk, B. H., "A Direct Measurement of the Most Probable Preferred Angular Velocity of Turbulent Structures by Optical Correlation of Laser Schlieren Signals," TM X-53870, 1969, NASA.